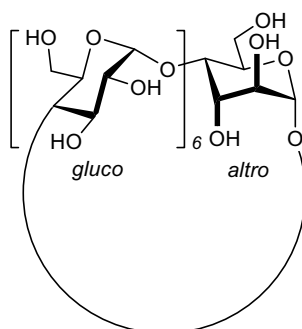


## Chapter 4

### Mono-*altro*- $\beta$ -cyclodextrin



#### Guest-induced Conformational Change in a Flexible Host: Mono-*altro*- $\beta$ -cyclodextrin

K. Fujita, W.-H. Chen, D.-Q. Yuan, Y. Nogami, T. Koga, T. Fujioka, K. Mihashi, S. Immel, and F. W. Lichtenthaler, *Tetrahedron: Asymmetry* **1999**, *10*, 1689-1696.





Pergamon

Tetrahedron: *Asymmetry* 10 (1999) 1689–1696

---

---

**TETRAHEDRON:  
ASYMMETRY**

---

---

## Guest-induced conformational change in a flexible host: mono-*altro*- $\beta$ -cyclodextrin<sup>†</sup>

Kahee Fujita,<sup>a,\*</sup> Wen-Hua Chen,<sup>a</sup> De-Qi Yuan,<sup>a</sup> Yasuyoshi Nogami,<sup>b</sup> Toshitaka Koga,<sup>b</sup>  
Toshihiro Fujioka,<sup>c</sup> Kunihide Mihashi,<sup>c</sup> Stefan Immel<sup>d</sup> and Frieder W. Lichtenthaler<sup>d,\*</sup>

<sup>a</sup>*Faculty of Pharmaceutical Sciences, Nagasaki University, Bunkyo-machi, Nagasaki 852-8131, Japan*

<sup>b</sup>*Daiichi College of Pharmaceutical Sciences, Tamagawa-cho, Minami-ku, Fukuoka 815, Japan*

<sup>c</sup>*Faculty of Pharmaceutical Sciences, Fukuoka University, Nanakuma, Fukuoka 814-0180, Japan*

<sup>d</sup>*Institut für Organische Chemie, Technische Universität Darmstadt, Petersenstrasse 22, D-64287 Darmstadt, Germany*

Received 10 March 1999; accepted 1 April 1999

---

### Abstract

Mono-*altro*- $\beta$ -cyclodextrin **1**, a  $\beta$ -cyclodextrin with one of the seven glucose units being configurationally changed to an altrose, is shown to be a flexible host undergoing a distinct conformational change within its altropyranose geometry upon intracavity inclusion of adamantanecarboxylate, thus representing an induced-fit model of binding rather than one following the rigid lock-and-key type pattern. © 1999 Elsevier Science Ltd. All rights reserved.

---

### 1. Introduction

In the common cyclodextrins, the six ( $\alpha$ -CD), seven ( $\beta$ -CD), and eight  $\alpha(1\rightarrow4)$ -linked glucose units ( $\gamma$ -CD)<sup>2</sup> are ‘locked up’ in a strait-jacket type belt,<sup>3–5</sup> so that their macrocycles exhibit remarkable structural rigidity: the glucopyranose rings inevitably adopt the energetically favorable <sup>4</sup>C<sub>1</sub> chair form, and the very limited rotational movements about the interglucosidic links, at best, allow one glucose unit to rotate out of the tilt of the others.<sup>5,6</sup> This pronounced rigidity even persists on inclusion-complex formation with a large structural variety of guests, since no significant guest-induced conformational changes have ever been observed.<sup>7</sup> Accordingly, the formation of inclusion complexes by  $\alpha$ -,  $\beta$ - and  $\gamma$ -CD closely corresponds to Emil Fischer’s classic lock-and-key concept for enzyme specificity,<sup>8</sup> i.e. to the insertion of a lipophilic key into an equally lipophilic cyclodextrin molecular lock. Although this process is overly static, it has nevertheless been extensively exploited towards ‘artificial enzymes’ or enzyme

---

\* Corresponding authors. E-mail: fujita@net.nagasaki-u.ac.jp and fwlicht@sugar.oc.chemie.tu-darmstadt.de

<sup>†</sup> Part 20 of the series *Molecular Modeling of Saccharides*. Part 19.<sup>1</sup>

models.<sup>9</sup> On the other hand, however, there is overwhelming evidence that the majority of enzymes act in an ‘induced fit’ fashion,<sup>10,11</sup> implying the induction of significant conformational changes in the enzyme upon ‘docking’ of the substrate — a dynamic process essential for the catalytic groups to assume the required transition state geometry. Hence, if low molecular weight cyclodextrins are to be *realistic* enzyme models, flexibility has to be introduced into their macrocycles so that they can mimic the dynamic induced-fit mode of action rather than the stationary lock-and-key approach.

With these considerations in mind, we have undertaken a study of the inclusion complexation properties of cyclodextrins in which one,<sup>12,13</sup> two,<sup>14</sup> or essentially all glucose units<sup>15–17</sup> — by inversion of their configuration at C-2 and C-3 — have been converted into altropyranose residues, which have been shown by calculation<sup>18</sup> and NMR evidence<sup>19</sup> to be conformationally flexible within the  ${}^4C_1 \rightleftharpoons {}^0S_2 \rightleftharpoons {}^1C_4$  pseudorotational itinerary (Fig. 1). As a result we report here on the inclusion of adamantane-1-carboxylate into mono-*altro*- $\beta$ -cyclodextrin **1**, representing — to the best of our knowledge — the first example of a guest-induced fit into a cyclooligosaccharide host.

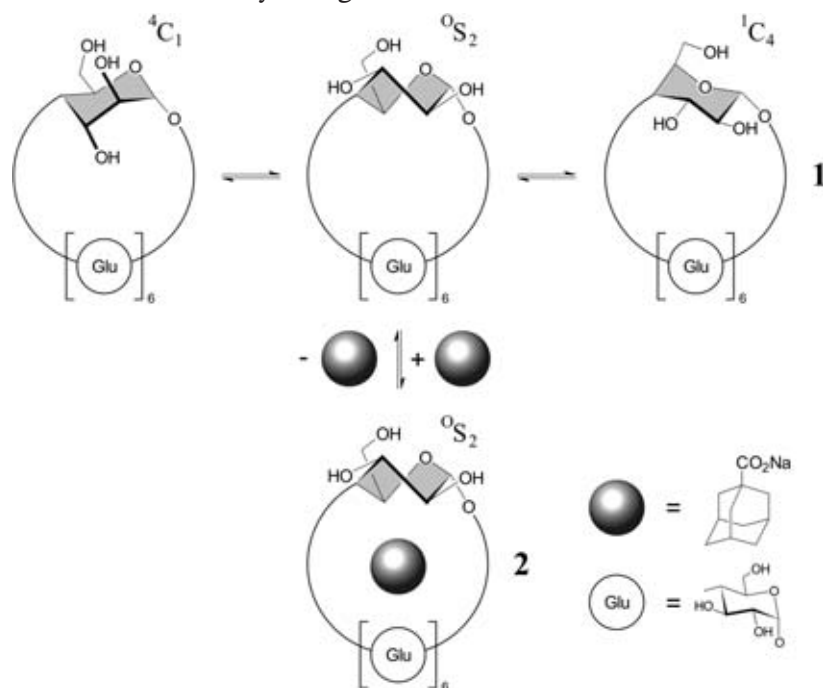


Figure 1. Schematic representation of mono-*altro*- $\beta$ -cyclodextrin **1** with its altropyranoid unit in  ${}^4C_1$ ,  ${}^0S_2$ , and  ${}^1C_4$  conformation, respectively, and its adamantanecarboxylate inclusion complex **2** in which the altrose residue is induced to preferentially adopt the  ${}^0S_2$  form

## 2. Results and discussion

Mono-*altro*- $\beta$ -CD **1**,<sup>2</sup> readily accessible from  $\beta$ -CD in a 3-step sequence,<sup>13,20</sup> shows distinct NMR signals for all of its protons (Fig. 2) from which the altrose hydrogens and their couplings could be identified either directly (H-1, H-5,  $J_{1,2}$ ), or by use of H–H COSY, homo-decoupling and 1D–HOHANA techniques (H-2–H-4,  $J_{2,3}$ – $J_{4,5}$ ). Comparison of the coupling constants thus determined with those calculated for  $\alpha$ -D-altropyranoid rings in idealized  ${}^4C_1$ ,  ${}^0S_2$ , and  ${}^1C_4$  conformations clearly reveals the altrose portion in **1** to essentially be in an  ${}^0S_2 \rightleftharpoons {}^1C_4$  equilibrium with an approximate 2:1 preponderance

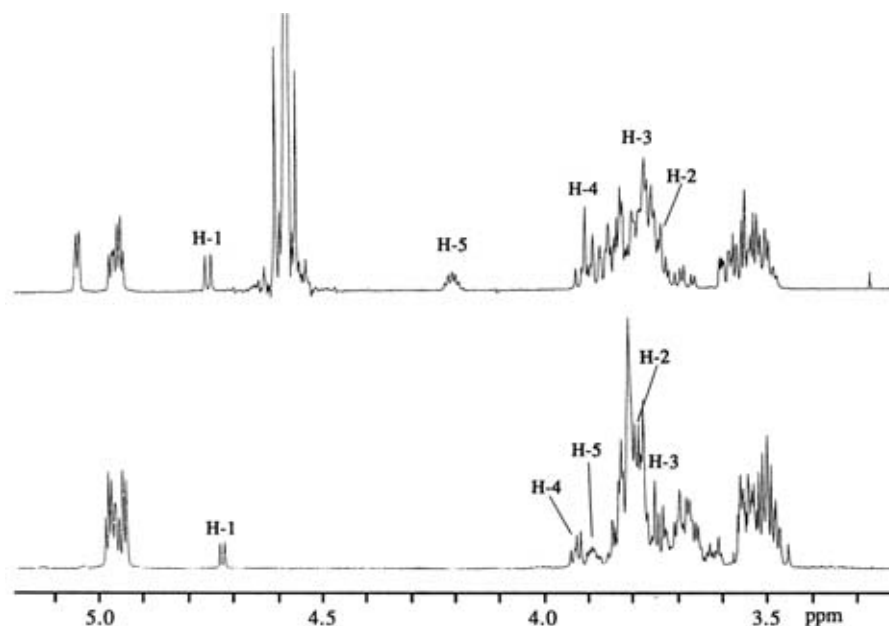


Figure 2. 500 MHz  $^1\text{H}$  NMR spectra of mono-*altro*- $\beta$ -cyclodextrin **1** (top), and of its adamantanecarboxylate inclusion complex **2** (bottom, 90% binding) in  $\text{D}_2\text{O}$  at  $35^\circ\text{C}$ . The altopyranose ring hydrogens are marked

of the  $^1\text{C}_4$  form. The exact positioning of the equilibrium between the three forms can most readily be inferred from the triangle representation in Fig. 3 (top entry), where the experimental coupling constants exhibit a best fit at a composition of 61%  $^1\text{C}_4$ , 31%  $^0\text{S}_2$ , and 8%  $^4\text{C}_1$  form — not surprising as the coupling constants found for **1** and those calculated for the  $^4\text{C}_1$  form (cf. Table 1) are indeed drastically different. That the  $^4\text{C}_1$  conformation is substantially under-represented in this equilibrium may be rationalized on the fact that it extends its axially oriented 3-OH into the interior of the mono-*altro*- $\beta$ -CD cavity, thereby causing steric hindrance as well as an interruption of the prevailing intra- and intermolecular hydrogen bond patterns.

For an assessment of the overall molecular shape of **1**, its cavity dimensions, and its potential for the formation of inclusion compounds, the molecular contact surface was generated (Fig. 4) as well as its molecular lipophilicity profile (Fig. 5), based on MD simulations in water. Accordingly, the altrose residue of **1** in water invariably adopts the  $^0\text{S}_2$  geometry (top pyranose unit in Fig. 4), entailing a solvent-accessible surface in slight elliptical distortion with a distinct cavity. In that, the overall shape of **1** closely resembles that of  $\beta$ -CD,<sup>21</sup> hence, should be capable of serving as host for guests featuring the adamantane moiety, as these represent perfect fits for  $\beta$ -CD.<sup>22</sup> This prediction can also be made on the basis of the close similarity of the molecular lipophilicity patterns of  $\beta$ -CD<sup>21</sup> and **1** (Fig. 5), as both exhibit a distinctly hydrophilic (blue) 2-OH/3-OH face vs. a hydrophobic (yellow) 6- $\text{CH}_2\text{OH}$  side.

Indeed, adamantane-1-carboxylate, which forms a 1:1 inclusion complex with  $\beta$ -CD with the guest fully inserted into its cavity,<sup>22</sup> is capable of intracavity complexation by **1**: upon addition to a  $\text{D}_2\text{O}$  solution of **1**, the NMR signals of the altroside portion of **1** gradually change with respect to both chemical shifts and coupling constants. H-5 is shifted upfield by as much as 0.3 ppm (cf. Fig. 2), a substantial shielding by the guest, indicating this ring hydrogen is now being directed towards the interior of the cavity (rather than to the outside as in the preferred  $^1\text{C}_4$  form of the ‘empty’ host **1**). Following this shift by NMR titration provided an association constant for **2** of  $839 \text{ M}^{-1}$ .

As distinct as the guest-induced chemical shifts are the changes in the  $J_{\text{HCCH}}$  coupling constants of the

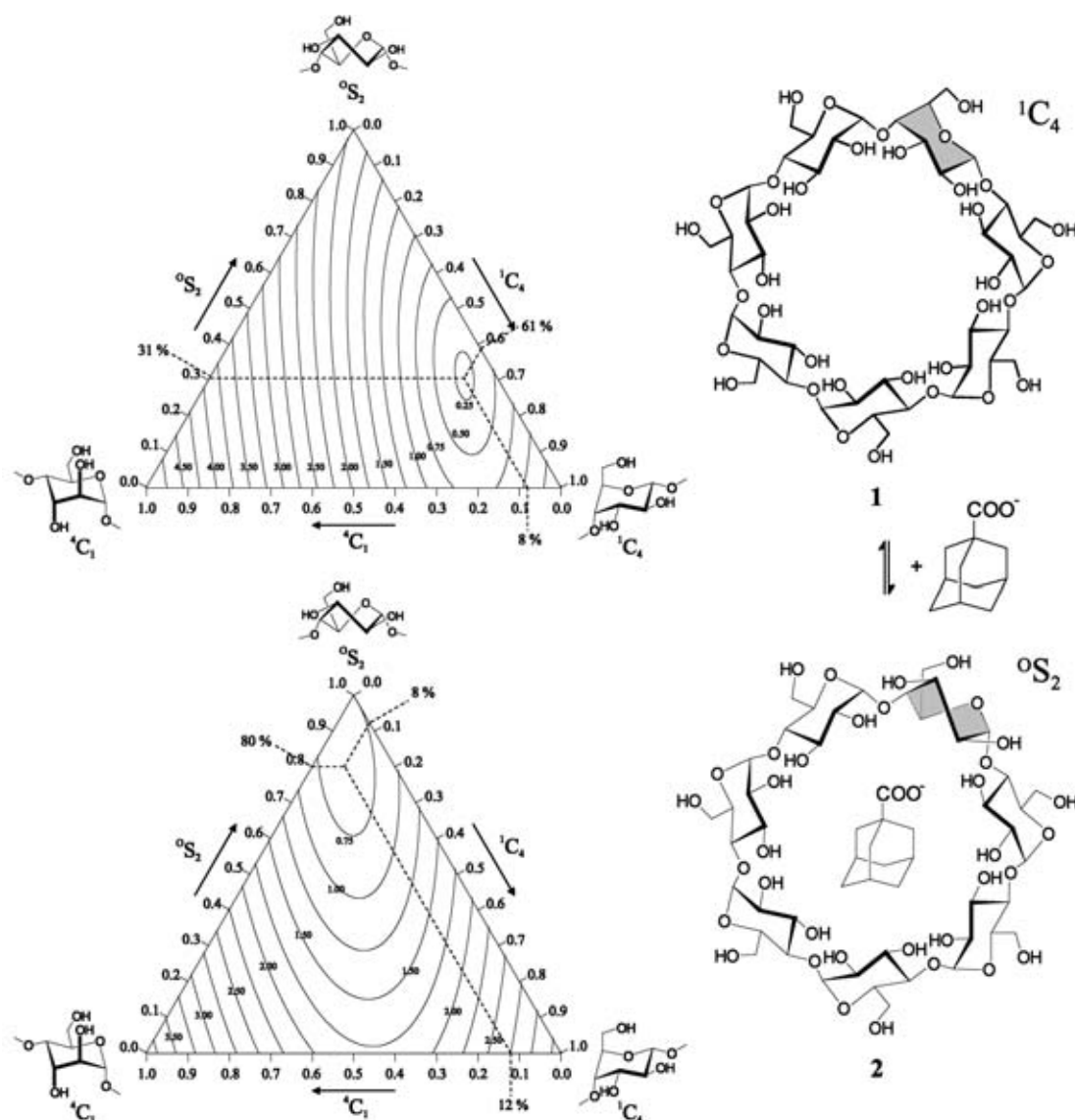


Figure 3. Triangular comparison of experimentally determined altopyranose ring couplings  $J_{1,2}$ ,  $J_{2,3}$ ,  $J_{3,4}$  and  $J_{4,5}$  (cf. Table 1) with those calculated for three-component equilibrium mixtures of the  ${}^4C_1$ ,  ${}^0S_2$ , and  ${}^1C_4$  forms. Contours signify the root mean-square deviation (i.e. the error  $\sigma$ ) between experimental data and those calculated for the three forms as a function of equilibrium composition, the contour minimum corresponding to the best fit attainable for the distribution of the individual conformers; contour levels are given in hertz within the range 0.25–4.5 Hz. The ‘empty’ mono-*altro*- $\beta$ -CD (**1**, top triangle) has its best fit at  $\sigma_{\min}=0.21$  Hz, corresponding to an equilibrium composition of the altopyranose conformations of 61%  ${}^1C_4$ , 31%  ${}^0S_2$ , and 8%  ${}^4C_1$ , i.e., in practical terms, to the presence of  ${}^0S_2$  and  ${}^1C_4$  forms in a 1:2 proportion. In the inclusion complex **2** (bottom triangle), the equilibrium is substantially shifted towards the  ${}^0S_2$  form (top triangle corner),  $\sigma_{\min}=0.61$  Hz implying an equilibrium composition of 12%  ${}^4C_1$ , 80%  ${}^0S_2$ , and 8%  ${}^1C_4$  form (i.e., the  ${}^0S_2$  form outweighs the others by 4:1)

altrose residue, most notably the doubling of  $J_{4,5}$  (from 3.5 to 7.0 Hz, cf. Table 1), while the others are influenced less extensively ( $J_{3,4}$  from 3.5 to 4.6 Hz) or not at all ( $J_{2,3}$ ). Comparison of the couplings found for **2** with those of the individual idealized altopyranose conformers (Table 1) clearly points towards the  ${}^0S_2$  form as the predominant geometry, or in terms of the triangle representation of the equilibrium

Table 1  
Vicinal  $^1\text{H}$ – $^1\text{H}$  coupling constants calculated for an  $\alpha$ -D-altropyranoid ring in idealized  $^4\text{C}_1$ ,  $^0\text{S}_2$ , and  $^1\text{C}_4$  conformations as compared to those found for mono-*altro*- $\beta$ -CD **1** and its adamantanecarboxylate inclusion complex **2**

$J$ (Hz)	Calcd <sup>a</sup> for ideal altropyranose geometries			Found for		Calcd <sup>b</sup> for 100 % <b>2</b>
	$^4\text{C}_1$	$^0\text{S}_2$	$^1\text{C}_4$	<b>1</b>	90 % <b>2</b> + 10 % <b>1</b>	
$J_{1,2}$	2.2	4.0	8.0	6.4	5.2	5.1
$J_{2,3}$	2.7	10.2	10.2	9.5	9.3	9.3
$J_{3,4}$	3.4	4.5	2.4	3.5	4.5	4.6
$J_{4,5}$	9.7	6.4	1.4	3.5	6.7	7.0

<sup>a</sup> Calculated according to the generalized Haasnoot-equation<sup>23</sup>

<sup>b</sup> Calculated for the fully developed inclusion complex with the experimental data for **1** and the inclusion equilibrium of 90 % **2** and 10 % **1**

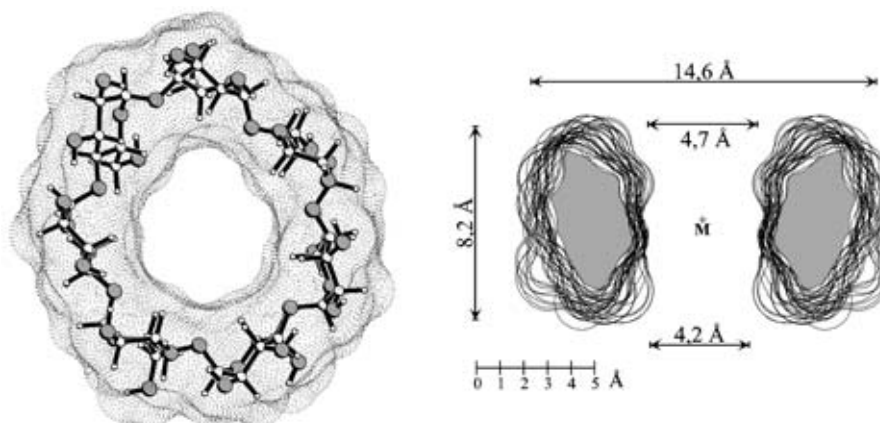


Figure 4. Ball-and-stick model of mono-*altro*- $\beta$ -CD (**1**) with the solvent-accessible surface superimposed in dotted form (left); the structure represents the mean geometry obtained from molecular dynamics simulations on **1** in water and subsequent energy minimization. In contrast to the glucose units (all  $^4\text{C}_1$ ), the altropyranose ring (top unit) adopts a  $^0\text{S}_2$  conformation; all pyranose rings are aligned almost perpendicular to the macrocycle mean-plane. The central cavity of **1** is only slightly elliptically distorted, and thus able to accommodate round shaped guest molecules like the adamantane carboxylate. On the right, the side-view cross-section cuts through the surface display the effective extension of the macrocycle and its cavity, with approximate molecular dimensions in Å

mixture to a composition of 12%  $^4\text{C}_1$ , 80%  $^0\text{S}_2$ , and 8%  $^1\text{C}_4$  (cf. Fig. 3). Hence, in essence, intracavity inclusion of adamantanecarboxylate into mono-*altro*- $\beta$ -CD results in a significant conformational change within the altrose portion, such that the  $^1\text{C}_4$  form predominating the equilibrium mixture in the ‘empty’ host is induced in the inclusion complex to shift to the  $^0\text{S}_2$  conformation which outweighs others by a factor of 4:1.

In summary, recourse to flexibility-modified cyclodextrins offers highly attractive lipophilic hosts for mimicking the dynamic induced-fit mode of enzyme action and thus has high potential for the design of realistic artificial enzymes. To this end, further inclusion complexation studies with the various di-*altro*-cyclodextrins<sup>14</sup> and the highly flexible cycloaltrins with six,<sup>15</sup> seven,<sup>16</sup> and eight<sup>17</sup>  $\alpha(1\rightarrow4)$ -linked altrose units are presently being pursued and shall be reported on in due course.

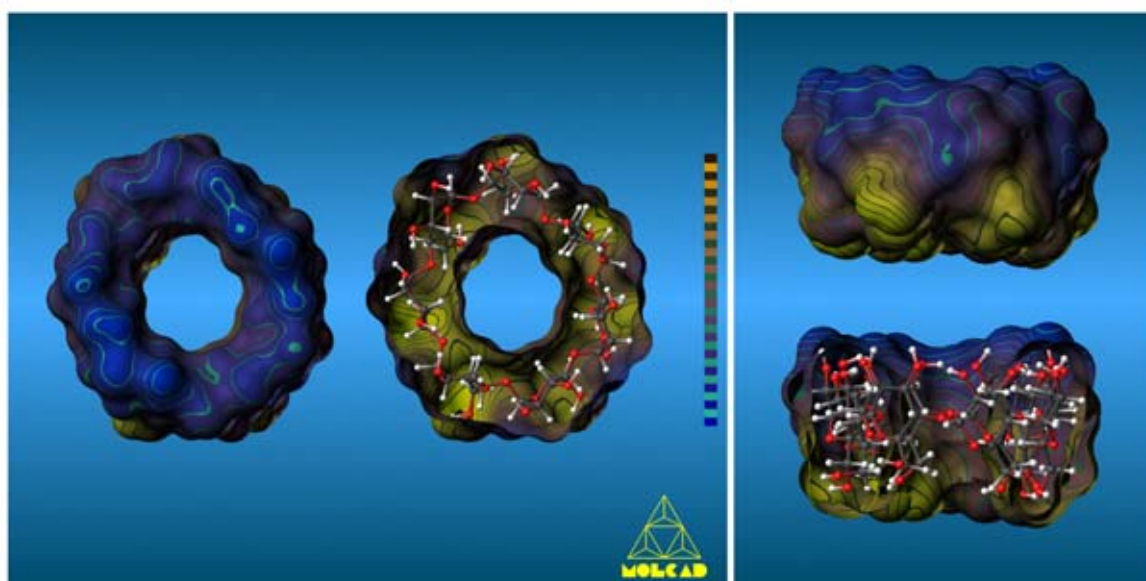


Figure 5. MOLCAD program-generated molecular lipophilicity patterns (MLPs) of **1**: the relative hydrophobicity on the molecular surface of **1** is visualized using a color-code ranging from dark blue (most hydrophilic areas) to yellow-brown (most hydrophobic regions). On the left, the intensively hydrophilic (blue) side of the macrocycle carries the 2-OH/3-OH groups; the half-opened surface with the ball-and-stick model insert displays the hydrophobic (yellow) surface regions around the 6-CH<sub>2</sub>OH groups. The right picture provides the side-view MLP of **1**, with closed and bisected surface representations exposing the shape and lipophilic characteristics of the central cavity as well as the most hydrophobic molecular regions around the primary 6-OH groups

### 3. Experimental

The NMR measurements were performed on a JEOL JNM A-500 spectrometer equipped with standard additions for H–H COSY homo-decoupling and HOHAHA techniques, whose application was necessary for determining in **1** the chemical shifts for the altrose ring protons H-2, H-3, H-4, and one of the H-6, as well as  $J_{2,3}$ ,  $J_{3,4}$  and  $J_{4,5}$ . For the inclusion complex **2**, only the chemical shift and  $J_{1,2}$  of the anomeric altrose proton can directly be extracted from the <sup>1</sup>H NMR spectrum; all other data (cf. Fig. 2 and Table 1) required recourse to H–H COSY and HOHAHA techniques as well as NOE experiments (irradiation with H-1).

The measurements of chemical shift changes as a function of concentrations (so-called NMR titrations) for determination of the association constant  $K$  followed standard methodology.<sup>24</sup>

Calculation of the molecular contact surfaces and the respective hydrophobicity potential profiles (MLPs) was performed using the MOLCAD<sup>25,26</sup> molecular modeling program and its texture mapping option.<sup>27</sup> Scaling of the MLP profiles was performed in relative terms (most hydrophilic to most hydrophobic surface regions); no absolute values are displayed.

### Acknowledgements

Support of this work by the Nihon Shokukin Kako (Japan Maize Products Co.) and the Fonds der Chemischen Industrie is gratefully acknowledged. Our thanks are also due to M.Sc. Yoshihiro Ikegami



for experimental assistance, and to Prof. Dr. J. Brickmann, Institut für Physikalische Chemie of the TUD, for providing us with his MOLCAD modeling software package.<sup>25</sup>

## References

1. Immel, S.; Schmitt, G. E.; Lichtenthaler, F. W. *Carbohydr. Res.* **1998**, *313*, 91–105.
2. The systematic name for **1** emerges from the most recent 'IUPAC Recommendations for the Nomenclature of Carbohydrates' (*Carbohydr. Res.* **1997**, *297*, 79, Rule 2-Carb-37.4.2) as *cyclo*[(1→4)- $\alpha$ -D-altropyranosyl-hexakis-(1→4)- $\alpha$ -D-glucopyranosyl], which, aside of being clumsy, implies it to be an assembly of 'glycosyls' rather than a 'glycoside', a heptasaccharide in fact. As semisystematic names, e.g. *cyclo*[mono- $\alpha$ (1→4)-D-*altro*-hexa- $\alpha$ (1→4)-D-gluco]-heptaoside for **1**, are equally impractical, we prefer the designation mono-*altro*- $\beta$ -CD as a reasonably descriptive, convenient acronym.
3. Szejtli, J. In *Comprehensive Supramolecular Chemistry*; Szejtli, J.; Osa, T., Eds. Chemistry, physical and biological properties of cyclodextrins; Elsevier: Oxford, 1996; Vol. 3, pp. 6–40. *Chem. Rev.* **1998**, *98*, 1743–1753.
4. Harata, K. In *Comprehensive Supramolecular Chemistry*; Szejtli, J.; Osa, T., Eds. Crystallographic studies of cyclodextrins; Elsevier: Oxford, 1996; Vol. 3, pp. 279–304. *Chem. Rev.* **1998**, *98*, 1803–1827.
5. Saenger, W.; Jacob, J.; Gessler, K.; Steiner, T.; Hoffmann, D.; Sanbe, H.; Koizumi, K.; Smith, S. M.; Takaha, T. *Chem. Rev.* **1998**, *98*, 1787–1802.
6. Szejtli, J. In *Comprehensive Supramolecular Chemistry*; Szejtli, J.; Osa, T., Eds. Inclusion of guest molecules, selectivity and molecular recognition by cyclodextrins; Elsevier: Oxford, 1996; Vol. 3, pp. 189–203. Fenyvesi, E.; Szente, L.; Russel, N. R.; McNamara, M. Specific guest types. *Ibid.*; Vol. 3, pp. 305–366.
7. Appreciable distortions of the glucopyranose <sup>4</sup>C<sub>1</sub> chair conformation have only been observed for the *m*-iodophenol inclusion complex of permethylated  $\beta$ -CD, in which one 2,3,6-tri-*O*-methyl-glucose residue adopts the <sup>0</sup>S<sub>2</sub> skew-boat form, see: Harata, K. *J. Chem. Soc., Chem. Commun.* **1988**, 928–929; and for permethyl  $\beta$ -CD monohydrate, in which one glucopyranoid ring—in the absence of a hydrophobic guest—is inverted to the <sup>1</sup>C<sub>4</sub> chair, see: Caira, M. R.; Griffith, V. J.; Nassimbeni, L. R.; van Oudtshoorn, B. *J. Chem. Soc., Perkin Trans. 2*, **1994**, 2071–2072.
8. Fischer, E. *Ber. Dtsch. Chem. Ges.* **1894**, *27*, 2985–2993. Lichtenthaler, F. W. *Angew. Chem.* **1994**, *106*, 2456–2467; *Angew. Chem., Int. Ed. Engl.* **1994**, *33*, 2364–2374.
9. Breslow, R. In *Inclusion Compounds*; Atwood, J. L.; Davies, J. E. D.; MacNicol, D. D., Eds. Enzyme models related to inclusion compounds; Academic Press: London, 1984; Vol. 3, pp. 473–508. Komiyama, M.; Shikegawa, H. In *Comprehensive Supramolecular Chemistry*; Szejtli, J.; Osa, T., Eds. Cyclodextrins as enzyme models; Elsevier: Oxford, 1996; Vol. 3, pp. 401–422. Breslow, R.; Dong, S. D. *Chem. Rev.* **1998**, *98*, 1997–2011.
10. Koshland Jr., D. E. *Angew. Chem.* **1994**, *106*, 2368–2372; *Angew. Chem., Int. Ed. Engl.* **1994**, *33*, 2375–2378.
11. Gerstein, M.; Lesk, A. M.; Clothia, C. *Biochemistry* **1994**, *33*, 6739–6749.
12. Fujita, K.; Nagamura, S.; Imoto, T. *Tetrahedron Lett.* **1984**, *24*, 5673–5676.
13. Fujita, K.; Ohta, K.; Ikegami, Y.; Shimada, H.; Tahara, T.; Nogami, Y.; Koga, T.; Saito, K.; Nakajima, T. *Tetrahedron Lett.* **1994**, *35*, 9577–9580.
14. Ohta, K.; Fujita, K.; Shimada, H.; Ikegami, Y.; Nogami, Y.; Koga, T. *Chem. Pharm. Bull.* **1997**, *45*, 631–635.
15. Nogami, Y.; Nasu, K.; Koga, T.; Ohta, K.; Fujita, K.; Immel, S.; Lindner, H. J.; Schmitt, G. E.; Lichtenthaler, F. W. *Angew. Chem.* **1997**, *109*, 1987–1991; *Angew. Chem., Int. Ed. Engl.* **1997**, *36*, 1899–1902.
16. Fujita, K.; Shimada, H.; Ohta, K.; Nogami, Y.; Nasu, K.; Koga, T. *Angew. Chem.* **1995**, *107*, 1783–1784; *Angew. Chem., Int. Ed. Engl.* **1995**, *34*, 1621–1622.
17. Nogami, Y.; Fujita, K.; Ohta, K.; Nasu, K.; Shimada, H.; Shinohara, C.; Koga, T. *J. Inclusion Phenom. Mol. Recogn. Chem.* **1996**, *25*, 53–56.
18. Angyal, S. J. *Aust. J. Chem.* **1968**, *21*, 2737–2746. Dowd, M. K.; French, A. D.; Reilly, P. J. *Carbohydr. Res.* **1994**, *264*, 1–19.
19. Lichtenthaler, F. W.; Mondel, S. *Carbohydr. Res.* **1997**, *303*, 293–302.
20. Ref. 12, footnote 8.
21. Lichtenthaler, F. W.; Immel, S. *Liebigs Ann. Chem.* **1996**, 27–37.
22. Hamilton, J. A.; Sabesan, M. N. *Acta Crystallogr., Sect. B* **1982**, *38*, 3063–3069. Lichtenthaler, F. W.; Immel, S. *Starch/Stärke* **1996**, *48*, 145–154.
23. Haasnoot, C. A. G.; De Leeuw, F. A. A. M.; Altona, C. *Tetrahedron* **1980**, *36*, 2783–2792.
24. Schneider, H.-J.; Hacket, F.; Rüdiger, Y. *Chem. Rev.* **1998**, *98*, 1768 ff., and literature cited therein.

1696

*K. Fujita et al. / Tetrahedron: Asymmetry 10 (1999) 1689–1696*

25. (a) Brickmann, J. *MOLCAD—MOLEcular Computer Aided Design*, Darmstadt University of Technology: Germany, 1996; *J. Chim. Phys.* **1992**, *89*, 1709–1721. (b) Waldherr-Teschner, M.; Goetze, T.; Heiden, W.; Knoblauch, M.; Vollhardt, H.; Brickmann, J. In *Advances in Scientific Visualization*; Post, F. H.; Hin, A. J. S., Eds. Springer: Heidelberg, Germany, 1992, pp. 58–67. (c) Brickmann, J.; Goetze, T.; Heiden, W.; Moeckel, G.; Reiling, S.; Vollhardt, H.; Zachmann, C.-D. In *Insight and Innovation in Data Visualization*; Bowie, J. E., Ed. Manning: Greenwich, UK, 1994; pp. 83–97.
26. Heiden, W.; Moeckel, G.; Brickmann, J. *J. Comp.-Aided Mol. Des.* **1993**, *7*, 503–514.
27. Teschner, M.; Henn, C.; Vollhardt, H.; Brickmann, J. *J. Mol. Graphics* **1994**, *12*, 98–105.